Effect of surface relaxations on the equilibrium growth morphology of crystals: platelet formation

Effect of surface relaxations on the equilibrium growth morphology of crystals: platelet formation

W T Lee, E K H Salje and Martin T Dove

Department of Earth Sciences, University of Cambridge, Downing Street,
Cambridge CB2 3EQ, UK

E-mail: `wlee@esc.cam.ac.uk`, `es10002@esc.cam.ac.uk` and `martin@esc.cam.ac.uk`

Abstract. In this paper we report results showing that surface relaxations may profoundly alter the equilibrium growth morphology of crystals. This may result in growth forms not predicted by the Wulff plot. Surface relaxations and polarization fluctuations produce extra terms in the free energy of a growing crystal nucleus which combine with the surface energy to produce an effective surface energy which depends on the size and shape of the crystal. We consider the case of the growth of nuclei of a crystal with cubic symmetry and show that if the surface relaxations are large enough then small nuclei will grow into platelets, although large nuclei still grow into large three-dimensional crystals. We show by considering materials with the perovskite structure that this effect may occur in real materials.

1. Introduction

In this work we investigate how two parallel surfaces of a small crystal can interact to produce platelet growth morphologies from crystals with cubic symmetry. The main interaction arises from the relaxation of the atomic layers parallel to the surface along directions normal to the surface, and for two close parallel surfaces the relaxation strain fields of both surfaces will overlap. This leads to a free energy that depends on the separation of the surfaces, and if the effect is large enough (or put another way, if the constant term in the surface energy is low enough) it can produce a symmetry breaking effect on the growth morphology allowing platelets to grow. Towards the end of the paper we estimate the size of the relaxation effect from experimental data for materials with the perovskite structure and show that it can be large enough to provide an explanation for platelet formation in real systems. We will contrast the results with other models of growth morphology.

This point of view is different from traditional models of nucleation and growth, which are based on the interaction of two terms in the free energy of a crystal nucleus. The first is the bulk free energy that drives the crystallization process. This term scales with the volume of the nucleus. The second term is surface energy. This term destabilizes small nuclei so that they dissolve. It scales with surface area. The interaction of the two terms leads to a critical nucleus size, beyond which a nucleus is large enough for the surface energy term not to destabilize it.

Crystalline solids are anisotropic. Because of this different surfaces have different surface energies depending on their (hkl) indices. The growth morphology of a crystal is determined from the condition that for a given crystal volume the total surface energy must be a minimum. A graph of the surface energy as a function of the direction of the normal of the surface is used

to determine equilibrium growth forms. Such a graph (or a two-dimensional slice from it) with the surface energy plotted in the direction of the normal of the surface is called a Wulff plot. The Wulff plots of most crystals have sharp cusps. The locations of these cusps correspond to planes with low Miller indices. The points of these cusps denote surfaces with very low surface energies. These surfaces are the ones that the crystal will use as its faces in order to minimize its surface free energy.

Obviously the symmetry of the Wulff plot must be at least the same as the point group symmetry of the crystal since surfaces related to each other by symmetry must have the same surface energy. Cusps must occur in symmetry related groups. One cusp implies the existence of others in directions related to that of the original cusp by the point group symmetry of the crystal. This means that the faces of a crystal must be related to each other by symmetry. For example, diamond, which as mentioned above forms octahedral crystals, has planes related by symmetry to the (111) plane as its lowest energy planes. To determine exactly the crystal growth morphology that will minimize the surface energy of a crystal from the Wulff plot a graphical construction called the Wulff construction is used. See for example Hartman (1973) for more information about the Wulff construction.

However crystals do sometimes grow in forms that are not consistent with the underlying symmetry of the lattice. For example silver halide crystals grow in a range of habits. As well as the cubic and cubic octahedral habits, which are consistent with the underlying cubic symmetry, tabular habits are also observed. These habits are explained as being due to twinning (Bögels *et al* 1997, 1999). In this paper we present results showing that equilibrium platelet growth may be brought about by a surface energy which depends on the separation of parallel surfaces

The Wulff plot contains assumptions about the nature of surface energies built into it. The most important of these assumptions is that the surface energy depends only on the Miller indices or the direction of the normal of the surface. Thermodynamically this must be true for sufficiently large crystals. The success of the Wulff plot in determining the growth morphologies of crystals indicates that this is often a good assumption. In this work we show that surface relaxations and polarization fluctuations in crystals result in terms in the free energy of a crystal that depend on the separation of parallel surfaces. Putting all the surface terms in the free energy together gives us an effective surface energy. In the limit of infinite thickness the effective surface energy tends towards the constant value used in the Wulff plot. Crystals grown from large nuclei will only experience the constant value of the surface energy and thus will grow into forms predicted by the Wulff plot. For crystals grown from small nuclei the effective surface energies may be substantially different from the Wulff plot values leading to entirely different growth morphologies.

The first person to suggest that surface energies may be modified by the size of a nucleus was Tolman (1949). He showed that as a consequence of the interface between a liquid drop and its vapour having a finite thickness the curvature of the surface would affect the surface energy. He derived a formula for the surface energy per unit area for a droplet of radius r:

$$\sigma(r) = \frac{\sigma_0}{1 + 2\delta/r}$$

where σ_0 is the surface energy per unit area for a flat surface, and δ is the Tolman length; a quantity of the order of the thickness of the interface. However δ is an extremely difficult quantity to measure experimentally and the temperature dependence and even the sign of δ are still the subject of debate (Baidakov and Boltachev 1999, Kalikmanov 1997, Granasy 1998). Although our results also involve a size dependent contribution to the free energy in our case it is due to the overlap of surface relaxations and polarization fluctuations rather than due to the curvature of the interface.

In this work we investigate surface effects in a one-dimensional slab. Firstly we look at how the presence of surfaces modifies the phonon density of states (section 2). We take the approach used in the rigid unit mode model for framework structures (Giddy *et al* 1993) to take explicit account of how the surface leads to a loss of constraints on the motions of surface atoms. This allows us to calculate the effect of the surface on the phonon density of states, and hence allows us to determine a temperature dependent phonon surface energy. This contribution to the surface energy scales directly with the surface area and so gives us the temperature dependence of surface energies.

Secondly we investigate the effects of surface relaxations on the surface free energy of the slab (section 3). Surface relaxations occur in systems where interactions between atoms in next nearest neighbour unit cells are important. In these systems atoms in the surface layers are not arranged in the same way as they are in the bulk because the forces on surface atoms are not the same as those on atoms in the bulk. The configuration of atoms in layers near to the surface that minimizes the free energy of the crystal is not the same as that of atoms in the bulk. The surface relaxation may be described by a strain field, which decays exponentially with distance from the surface. Strains are measured relative to a reference configuration in which atoms close to the surface are arranged in the same way as atoms in the bulk. The free energy change associated with a surface relaxation is negative. For small crystal nuclei the strain fields of surface relaxations from different surfaces overlap. In our one-dimensional slab surface relaxations from the opposite surfaces may overlap. When we calculate the contribution to the surface energy from the surface relaxation we obtain two terms. The first term is negative and scales directly with the surface area. The second term, as well as being proportional to the surface area has a decaying exponential dependence on the separation of the surfaces.

Lastly we consider the effect of polarization fluctuations in the crystal nucleus and in the medium surrounding it (section 4). These have already been studied in detail for slabs in the context of surface melting (Lipowsky 1987). It has been shown that polarization fluctuations make a contribution to the free energy that scales with the surface area and has, for slabs with a large thickness, a power law dependence on the thickness. In the surface melting case the free energy of the molten layer has both a term which depends exponentially on its thickness and a term which at large thickness has a power law dependence on the thickness. In this case for small thickness the exponential term dominates and for large thickness the power law term dominates. We expect the same thing to happen in our system. However as we discuss in the next section, whether or not a platelet growth morphology can occur depends on the form of the surface energy for small values of thickness. Therefore we do not expect the polarization term to have a role in modifying the growth morphologies of crystals.

In section 5 we extrapolate our results for the free energy of a slab to the case of a rectangular parallelepiped nucleus. We investigate the form of this function and its stationary values. In section 6 we discuss what growth morphologies it can produce. We consider the possibilities of cubic, platelet and needle growth morphologies. We find, as expected, that the possibility of a cubic growth morphology always exists. Needle growth cannot occur under any of the circumstances we consider. Platelet growth may occur but depends on the initial shape of the nucleus, and the behaviour of the surface energy for small values of thickness.

Having determined the conditions necessary for platelet growth morphologies we explore the question of whether we can reasonably expect the effect to occur in real systems. Because the condition for platelet growth morphologies depends on the behaviour of the surface energies for nuclei with small thickness this means only the surface relaxation contribution to the surface energy is important. In section 7 we consider the parameters of the surface relaxations of materials with the perovskite structure. Here our aim is not to demonstrate that the platelet formation mechanism may be applicable to these materials. Instead we investigate whether

the parameters of surface relaxations in real systems are the right order of magnitude for the platelet formation mechanism to work. Our results suggest that this is indeed the case.

2. Phonon surface free energy

In this section we look at the effect that the surface has on the phonon spectrum and how the free energy is affected. We do this firstly by investigating how creating a surface increases the number of low frequency phonon modes. The effect of a surface is to reduce the forces constraining surface atoms to their places. This allows them to move more easily (that is with less potential energy cost) than bulk atoms. This will lower the frequency of phonons whose eigenvectors involve the motion of those atoms. The lowering of the frequency of the phonon mode will lower the energy of the phonons in the mode. The number of phonons occupying the phonon mode is given by Bose–Einstein statistics (see for example Dove 1993, Landau and Lifshitz 1980)

$$N(\omega) = \frac{1}{\exp(\omega/T) - 1}.$$

Decreasing the frequency of the phonon mode will increase the number of phonons occupying the mode. The increase in the total number of phonons will lead to an increase in the entropy of the system. Thus, through $A = E - TS$, the free energy of the system will be lowered by the presence of surfaces. This is compared to the same system but with periodic boundary conditions.

Put more simply, the role of the surface will be to remove some of the constraints on the motions of the surface atoms. This is conveniently analysed using the rigid unit mode (RUM) model, which is explicitly based on the balance between the number of constraints and the number of degrees of freedom of a system containing rigid polyhedra (such as the octahedra in the perovskite structure) that are linked together. This model has been successfully used to explain many features of phase transitions in silicates and other ceramics (Hammonds *et al* 1996, Dove *et al* 1995). It has been extended to give an explanation of negative thermal expansion in ceramics such as ZrW_2O_8 (Pryde *et al* 1996, 1998) and silicates such as quartz (Welche *et al* 1998), zeolite catalysis (Hammonds *et al* 1997, 1998) and the low energy dynamics of silica glass (Dove *et al* 1997, Trachenko *et al* 1998).

RUMs are a special class of phonon modes, and are defined as the phonon modes with eigenvectors that do not involve any distortion of the structural polyhedra (such as SiO_4 tetrahedra or TiO_6 octahedra) themselves, with the polyhedra effectively moving as rigid units. Because there is a high energy cost involved in distorting these structural polyhedra, the RUMs will have lower frequencies than other phonons and will accordingly make a larger contribution to the free energy. Therefore to a first approximation the free energy of a system will be proportional to the number of RUMs in the system. This will be exactly valid in the limit that the frequency of a RUM is much less than the frequency of all other phonon modes. If we suppose that all RUMs have frequencies of approximately ω_{RUM} and the system has N_{RUM} RUMs then the free energy of the system will be approximately

$$N_{RUM} T \ln \left[1 - \exp \left(- \frac{\omega_{RUM}}{T} \right) \right].$$

At this level of approximation we can deduce the effect of the surfaces on the free energy by calculating the effect of the surfaces on the number of RUMs.

The effect of the surface on the number of RUMs is explained most easily with reference to some general considerations. A system of linked polyhedra has a total of F degrees of freedom (actually six per polyhedron, three translational and three rotational). There will

also be a number of constraints, C, which act to tie together the corners of linked polyhedra. Specifically, one linkage adds three constraints to the overall count. The number of RUMs is equal to $F - C$ (Thorpe 1995). For a crystal made of linked tetrahedra the most general way of counting C leads to the result that $F - C = 0$, but this does not account for symmetry which will make some of the constraints degenerate, and it is found for many systems that symmetry allows a significant number of RUMs. A lattice dynamical method of determining the number of RUMs for a system with periodic boundaries has been described elsewhere (Giddy *et al* 1993, Hammonds *et al* 1994). This is a numerical method that automatically accounts for the effect of symmetry on the overall number of constraints. The issue of symmetry is discussed in more detail elsewhere (Giddy *et al* 1993, Dove 1997).

The effect of a surface is to leave some corners of surface polyhedra unconnected, reducing the number of constraints C by an amount that is proportional to the surface area. This increases the number of RUMs by the same amount. In our simplified model the free energy is proportional to the number of RUMs. The number of RUMs will be $AV + BS$, where V is the volume of the system and S is the surface area. A and B must be positive. This approach shows that there will be a bulk phonon free energy and a surface phonon free energy. There is a (negative) contribution to the free energy that is proportional to the surface area.

As part of this work we have investigated the effects of the presence of free surfaces on the number of RUMs and the crystal free energy on the following structure types: cubic perovskite, hexagonal tridymite, cubic cristobalite and cubic sodalite. These were chosen because they have quite different RUM behaviours. perovskite has lines of RUMs in k-space. Tridymite and cristobalite have planes of RUMs. Sodalite has at least one RUM at each point in k-space (Hammonds *et al* 1996). We created periodic supercells consisting of slabs of n primitive unit cells stacked in the c direction. We varied n between 2 and 20. The slabs have translational periodicity in the a and b directions, but have free (001) surfaces. We calculated the frequencies of the phonon modes at 1000 randomly chosen points in the effectively two-dimensional k-space.

In the limit of high temperatures the phonon free energy is given by

$$A = 6mT \left\langle \ln \frac{\omega}{T} \right\rangle.$$

The prefactor is 6 rather than 3 because we are dealing with rigid units with six degrees of freedom rather than atoms, which only have three degrees of freedom. m is the number of rigid units in the unit cell. Angular frequencies and temperatures are measured in energy units so $\hbar = 1$, $k_B = 1$.

The meaning of the average is given, for a structure of N unit cells, by

$$\left\langle \ln \frac{\omega}{T} \right\rangle = \frac{1}{6Nm} \sum_{i=1}^{6Nm} \ln \left(\frac{\omega_i}{T} \right).$$

Summation is over all the phonon modes of the system. There is no practical problem with calculating $\langle \ln \omega \rangle$ and subtracting $\ln T$ later.

The main problem with this approach is in handling the modes with zero frequency, since the free energy equation requires the logarithm of the frequency. In a real crystal the RUMs do not in fact have zero frequencies, just very low ones. Therefore we solved the problem by adding 0.5 THz to each frequency. (Note that the frequency range for the phonon modes in silicates, excluding the very high frequency modes involving stretching of bonds that are not reproduced in our calculation, is 0–20 THz.)

The results show that the free energy analysis of the RUM systems we have investigated shows that the free energy per unit volume varies with n as $A + B/n$. The first term scales
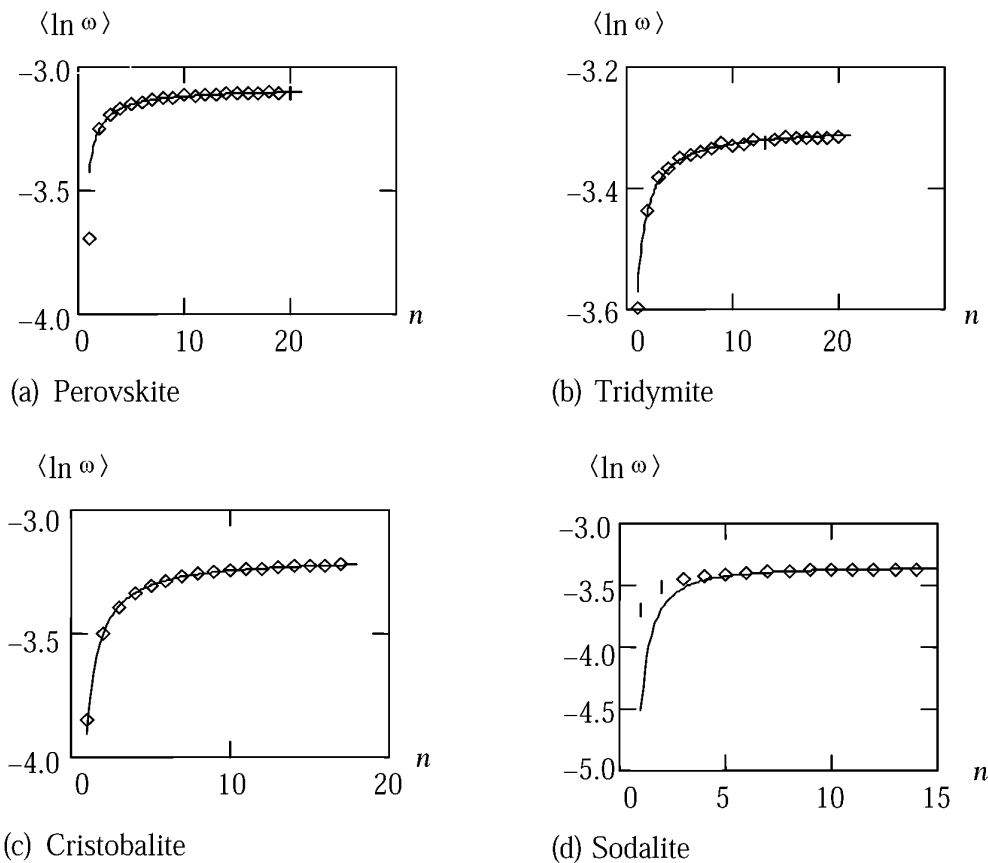
Figure 1. This figure shows the value of ⟨ln ω⟩ for each structure as a function of number of layers. Except in the case of perovskite where it was unnecessary 0.5 THz was added to each frequency to deal with the problem of zero frequencies. The diamonds are the values calculated. The lines are fits of the form $A + B/n$. As can be seen in each case the fit is good, except for the first few points on the sodalite curve.

with the volume of the system and gives the bulk phonon energy. The second term gives a contribution that scales with the surface size and gives the surface phonon free energy. In the cases of perovskite, tridymite and cristobalite fits of this form agree with the data very well and there is no evidence to support higher order terms in $1/n$. However in the case of sodalite there does appear to be a need for higher order terms. We show in figure 1 graphs of ⟨ln ω⟩ as a function of n for the structures mentioned above.

The surface contribution to the phonon free energy is:

$$\Delta\sigma = 6mT\beta\gamma.$$

The parameters are: m the number of rigid units in a unit cell, β the coefficient of $1/n$ in the expansion of ⟨ln ω⟩ as a power series in $1/n$, and γ the number of unit cells per unit area of surface. (Temperature is measured in energy units, i.e. $k_B = 1$.) We give values of these parameters for the substances in table 1.

The above results can easily be incorporated into the Wulff plot by allowing the surface free energy to vary with temperature. To obtain an idea of the size of the effect consider perovskite.

Table 1. Values of the parameters used for the calculation of the phonon surface free energies for the various mineral structures. For the perovskite structure γ is calculated using the lattice parameters of strontium titanate.

	m	β	γ (10^{18} m^{-2})
Perovskite	1	−0.328	6.6
High tridymite	4	−0.271	4.5
High cristobalite	8	−0.537	2.0
Sodalite	12	−0.212	1.3

Upon a temperature increase of 1000 K the surface energy decreases by 0.17 J m^{-2} (the lattice parameters of strontium titanate have been used).

Granzio and Uccio (1997) calculated the free surface energy of YBCO at zero Kelvin as $\sigma = 0.8$ J m^{-2} so this is quite a significant effect. In section 7 we show that small values of the surface energy are needed for platelet formation to occur. At high temperatures the phonon contribution to the surface energy may drive the surface energy below the critical value needed for platelet formation.

We note that these calculations were performed for perfectly smooth surfaces, which will not be a good representation of the situation in a growing crystal. The effect of rough surfaces can be determined qualitatively by the constraint counting method discussed above. Clearly a rough surface will have even less constraints than a smooth one. This in turn will give more RUM phonon modes that will lower the surface free energy of the system. For this reason the phonon contribution to the surface free energy may lower it even further than the above calculations suggest.
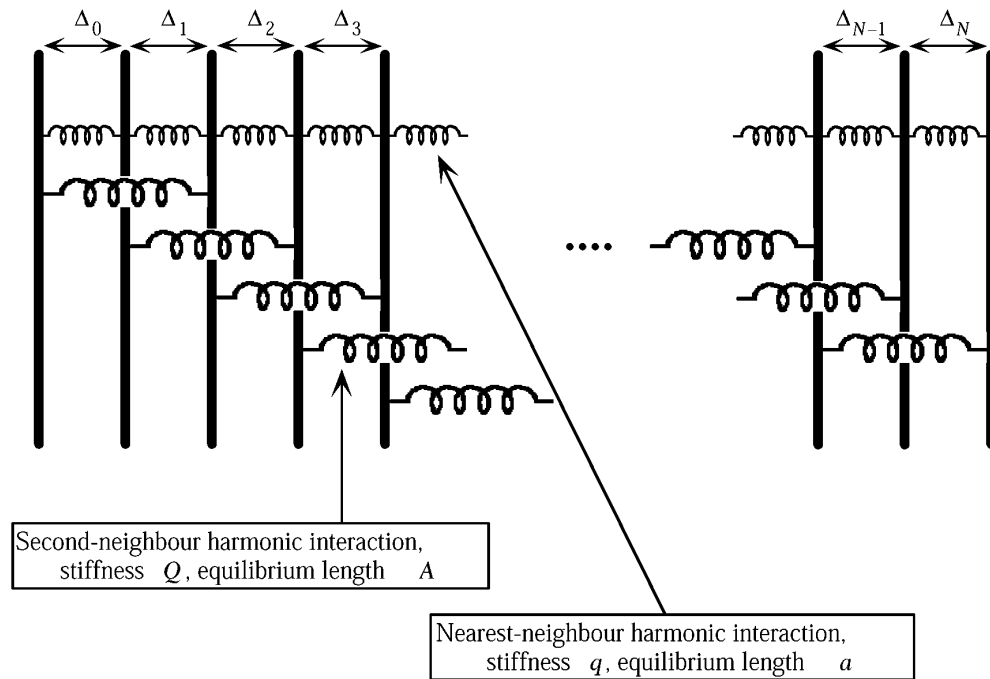
3. Surface relaxations

The presence of a surface allows the system to lower its free energy by changing its configuration, in a region near the surface, from its bulk configuration. This can be explained in terms of forces. In the bulk of the material the forces on any plane are balanced. When the material on one side of the plane is removed to create a free surface the force on that surface is no longer balanced, i.e. there is a net force on the surface. The new equilibrium state of the crystal has a region close to the surface which is strained with respect to the bulk. These strains decay exponentially in the bulk with length scale λ, the relaxation length. Note that to obtain this result from elasticity theory the elastic free energy must contain terms depending on the derivative of the strain, not just the strain itself.

The simplest model that shows surface relaxations is a set of crystallographic planes, as shown in figure 2. Nearest neighbour planes and next nearest neighbour planes are joined by springs (Houchmandzadeh *et al* 1992). Displacements are only allowed in one dimension.

We are interested in the case where the strain fields of relaxations emanating from each surface overlap. Nearest neighbour planes are joined by springs with equilibrium length a and spring constant q. Next nearest neighbour planes are joined by springs of equilibrium length A and spring constant Q. The separation of the planes is given by $\{\Delta_i\}$. Conditions of stability require $q > 0$ and $Q > -q/4$ (Houchmandzadeh *et al* 1992). Should these conditions be violated these systems show ferroelastic or antiferroelastic phase transitions, which may be viewed as cases where $\lambda \to \infty$. Thus systems which undergo such transitions have large values of λ close to their transition temperatures. In the bulk the separation of the lattice planes

Figure 2. The simplest system that has surface relaxations is a set of planes joined by springs. Both nearest neighbour and next nearest neighbour planes must be connected by springs in order for there to be a surface relaxation. The set $\{\Delta_i\}$ $i = 0, 1, \ldots, N$ is the separations of the planes.

is given by b:

$$b = \frac{qa + 2QA}{q + 4Q}.$$

The choice of parameters for the nearest and next nearest neighbour's spring constant determines the qualitative form of the relaxation (see previous reference). If $Q < 0$ then the strain decays purely exponentially, i.e. all the planes move in the same direction when the surface is allowed to relax. (Negative values of Q are physically possible, for instance if the interaction between planes is a Lennard-Jones type potential.) If $Q > 0$ then the strain has an exponential envelope but alternates in sign in each layer, i.e. adjacent atoms move in opposite directions. This sort of surface relaxation is called a zigzag relaxation.

The total energy of the system after relaxation may be calculated exactly, and the bulk energy (that of the unrelaxed system) can be subtracted off to leave a surface energy. The surface relaxation energies are different in the cases $Q > 0$ and $Q < 0$. We give the results for $\lambda \gg 1$ (λ is measured in unit cell lengths); they are first order in the displacements and only the first exponential term is kept. We give the derivation of these in appendix A. The exponential term for relaxations with $Q > 0$ alternates in sign with N, but in our model of equilibrium growth, given in the next section, we assume that the system only feels the envelope. The sign of the exponential term is taken to be negative all the time.

$$Q < 0$$

$$\lambda = \sqrt{-\frac{Q}{q + 4Q}}$$

$$\Delta V = -\frac{2Q^2(2b-A)^2}{[q+2Q-Q/\lambda]} + \frac{4Q^3(2b-A)^2}{\lambda[q+2Q-Q/\lambda]^2} \exp\left(-\frac{N}{\lambda}\right)$$

$$Q > 0$$

$$\lambda = \sqrt{\frac{Q}{q}}$$

$$\Delta V = -\frac{2Q^2(2b-A)^2}{[q+2Q/\lambda]} - \frac{4Q^3(2b-A)^2}{\lambda[q+Q/\lambda]^2} \exp\left(-\frac{N}{\lambda}\right).$$

As mentioned above in the $Q > 0$ case the exponential term alternates in sign with the addition of each layer and should be multiplied by $(-1)^N$. To see why this is the case consider the overlap of two zigzag relaxations emanating from two surfaces. In order for them to interfere constructively, N, the number of planes in the chain, must be even. This case will have lower energy than the case where N is odd and the two relaxations interfere destructively.

The exponential terms depend on the separation between the surfaces, and so cannot be incorporated into the Wulff plot.

Values for the parameters used can be calculated from interatomic potentials. In this work rough values are estimated from experimental and theoretical data to see whether the effects due to the surface relaxation described in section 6 are likely to occur.

4. Polarization effects

In this section we consider the effects of van der Waals interactions. These have been studied in the context of surface melting phenomena (Lipowsky 1987, 1985, Conrad 1992) and wetting (Lipowsky 1985, Widom 1978). Surface melting occurs in some metals at temperatures just below the melting temperature. A thin disordered layer forms on the surface. The free energy of a liquid layer of thickness z can be calculated using the Landau theory of first order phase transitions (Lipowsky 1987)

$$A(z) = \gamma_{SL} + \gamma_{LV} + z\Lambda + (\gamma_{SV} - \gamma_{SL} - \gamma_{LV}) \exp\left(-\frac{2z}{\lambda}\right)$$

where γ_{SL} is the surface energy of the solid–liquid interface, γ_{LV} is the surface energy of the liquid–vapour interface and γ_{SV} is the surface energy of the solid–vapour interface. Λ is the excess free energy of bulk liquid compared to bulk solid and λ is the correlation length of the liquid. The above form of the free energy is valid for small values of z where the free energy of the interface is dominated by short range interactions. For larger values of z long range van der Waals interactions become important. Van der Waals interactions are due to correlated fluctuations in electrical polarization. For two atoms separated by a large distance r their van der Waals interaction energy is given by $-\varepsilon(\lambda/r)^6$ if retardation effects are neglected.

For condensed bodies the van der Waals interaction is more complicated than this. The van der Waals energy per unit area of a slab suspended in some medium is given by Wz^{-2} where W is the Hamaker constant. Again retardation effects are neglected. For a monatomic liquid layer on a solid surface W is given by

$$W = \frac{\pi}{12} n_L(n_S - n_L)\varepsilon\lambda^6.$$

n_S and n_L are the number densities of atoms in the solid and liquid respectively. ε and λ are the parameters of the two-atom interaction. If the solid is denser than the liquid, as is usually the case, W will be positive. However in general W can have either sign. So for large values

of $zA(z)$ is given by

$$A(z) = \gamma_{SL} + \gamma_{LV} + z\Lambda + (\gamma_{SV} - \gamma_{SL} - \gamma_{LV})\exp\left(-\frac{2z}{\lambda}\right) + \frac{W}{z^2}.$$

The crossover between these two types of behaviour has been observed experimentally (Pluis *et al* 1989).

In our system, which consists of a solid slab in contact with a liquid or vapour, we expect polarization contributions to the surface energy to be important when the system is large enough. For a solid slab suspended in a liquid the Hamaker constant is given by $W = -(\pi/12)(n_L - N_S)^2\varepsilon\lambda^6$ (Lipowsky 1985). We expect the surface energy therefore to be given by

$$\sigma(z) = \sigma_0 + f(z)$$

$$\lim_{z\to 0} f(z) \propto \exp\left(-\frac{z}{\lambda}\right)$$

$$\lim_{z\to\infty} f(z) \propto \frac{1}{z^2}.$$

However as we demonstrate in section 6 it is the properties of the surface energy for small values of z that determine whether a change in the growth morphology occurs or not. Therefore changes in the growth morphology are entirely attributable to the surface relaxation and not to polarization effects.

5. Free energy of a nucleus

In this section we consider how to extend our results for a slab, a one-dimensional problem, to the case of a growing crystal nucleus, a three-dimensional system. We consider nuclei with {001} type surfaces. The resultant free energy may be interpreted as having a bulk term and a surface term as before. However as a result of polarization and surface relaxations contributions to the surface energy it no longer dependent solely on the surface area but also on the separation of opposite surfaces. We investigate the behaviour of the free energy as a function of the size and shape of nuclei for a general surface energy, which increases monotonically to a (positive) constant value as a function of the separation of surfaces.

We consider the free energy of the nucleus of a faceted crystal of the cubic system. We assume for simplicity that the Wulff plot of the crystal is such that we only need to consider surface planes related to the (001) plane by cubic symmetry. Such a crystal will be a rectangular parallelepiped with edge lengths x, y and z. Ignoring polarizations and surface relaxations the free energy of the nucleus will be

$$A(x, y, z) = 2\sigma(xy + yz + zx) - \theta xyz$$

where σ is the local surface energy per unit area for an (001) surface and θ is the bulk free energy per unit volume. If the non-local contribution to the surface energy per unit area of a slab from polarizations and surface relaxations is $f(L)$ then the full free energy of a nucleus will be

$$A(x, y, z) = 2\sigma(xy + yz + zx) + xyf(z) + yzf(x) + zxf(y) - \theta xyz.$$

For simplicity we can choose our units of energy so that 2σ is one. This gives us

$$A(x, y, z) = (xy + yz + zx) + xyf(z) + yzf(x) + zxf(y) - \theta xyz. \tag{1}$$

In the discussion below we assume that $f(x)$ is a monotonically increasing function. $f(0)$ is negative but finite and as x approaches infinity $f(x)$ monotonically approaches zero. This will be the case when the Hamaker constant (discussed in section 4) is negative.

We look for points at which $A(x, y, z)$ is stationary and discuss the expansion of the function about those points. It can be shown that the stationary points of A satisfy the relation

$$\frac{A(x, y, z)}{xyz} = f'(x) - \frac{f(x)}{x} - \frac{1}{x} = f'(y) - \frac{f(y)}{y} - \frac{1}{z} = f'(z) - \frac{f(z)}{z} - \frac{1}{z}.$$

The equation $f'(a) - f(a)/a - 1/a = \text{const}$ may have one, two or three solutions depending on the value of the constant and the form of $f(x)$. If the form of $f(x)$ is known then the above equation can be used to determine the possible location of stationary values.

We investigate further the stationary values of A and their expansion along the line $x = y = z$. Stationary points along this line are given by

$$0 = 2x(1 + f(x)) + x^2(f'(x) - \theta).$$

One solution is obviously at $x = 0$. The number of other solutions depends on the exact form of $f(x)$. The number of other stationary values depend on the exact form of $f(x)$. They are summarized in table 2 and graphs of $A(x, x, x)$ are shown in figure 3.

Table 2. The number of stationary values of $A(x, y, z)$ along the $x = y = z$ line depends on the exact form of the size dependent part of the surface energy $f(x)$. This table summarizes the conditions necessary for there to be one, two and three stationary values along that line.

Number of stationary values along the line $x = y = z$	Condition(s)
1	$1 + f(0) < 0$
	$\max[2(1 + f(a)) + a(f'(a) - \theta)] < 0$
2	$1 + f(0) > 0$
3	$1 + f(0) < 0$
	$\max[2(1 + f(a)) + a(f'(a) - \theta)] > 0$

To determine the nature of these stationary values we find the (quadratic) expansion of A about these points. The expansion of $A(x, y, z)$ about a stationary point at (x, y, z) is given by
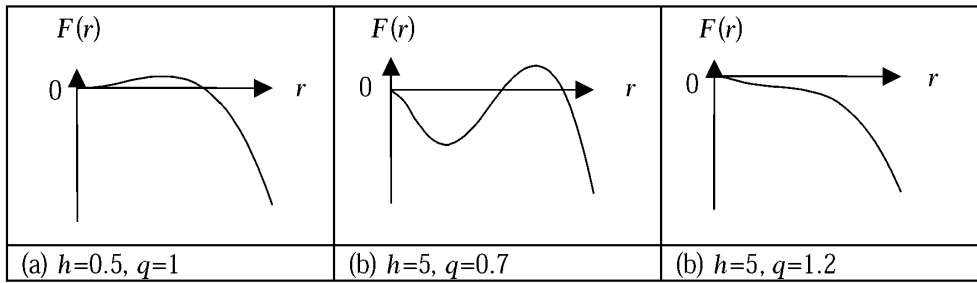
$$A(x + \Delta x, y + \Delta y, z + \Delta z) - A(x, y, z)$$

$$= \frac{1}{2}[\Delta x \, \Delta y \, \Delta z] \begin{bmatrix} \dfrac{\partial^2 A}{\partial x^2} & \dfrac{\partial^2 A}{\partial x \partial y} & \dfrac{\partial^2 A}{\partial x \partial z} \\ \dfrac{\partial^2 A}{\partial y \partial x} & \dfrac{\partial^2 A}{\partial y^2} & \dfrac{\partial^2 A}{\partial y \partial z} \\ \dfrac{\partial^2 A}{\partial z \partial x} & \dfrac{\partial^2 A}{\partial z \partial y} & \dfrac{\partial^2 A}{\partial z^2} \end{bmatrix} \begin{bmatrix} \Delta x \\ \Delta y \\ \Delta z \end{bmatrix}.$$

The above matrix can be diagonalized by a co-ordinate transformation. The diagonal elements of the matrix are then its three eigenvalues. In the case where $x = y = z$ the matrix of the quadratic form is diagonalized in a cylindrical polar co-ordinate system (ξ, ζ, ψ). ξ is a coordinate along the $x = y = z$ line and ζ is a coordinate directed perpendicular to this line; ψ is the angle in the plane perpendicular to the $x = y = z$ direction. The expansion of $A(x, y, z)$ about a stationary point at (x, x, x) is given by

$$A = A_0 + \frac{\lambda_\xi}{2}\xi^2 + \frac{\lambda_\zeta}{2}\zeta^2$$

$$\lambda_\xi = \frac{\partial^2 A}{\partial x^2} + 2\frac{\partial^2 A}{\partial x \partial y}$$

$$\lambda_\zeta = \frac{\partial^2 A}{\partial x^2} + 2\frac{\partial^2 A}{\partial x \partial y}$$

(a) $h=0.5$, $q=1$	(b) $h=5$, $q=0.7$	(b) $h=5$, $q=1.2$

Figure 3. This figure shows the free energy of a cubic nucleus as a function of edge length r. As shown, which of the three possible shapes the curve has is determined by the values of the two parameters η and θ. (a) Case 1, a minimum at the origin and a maximum. (b) Case 2, a maximum at the origin followed by a minimum then a maximum. (c) Case 3, a single maximum at the origin. As is noted in the text in cases 2 and 3 cubic nuclei do not necessarily remain cubic as they grow so these graphs do not provide a complete picture of the nucleation and growth of nuclei.

$$A_0 = A(x, x, x)$$
$$\left.\frac{\partial^2 A}{\partial x^2}\right|_{(x,x,x)} = x^2 f''(x)$$
$$\left.\frac{\partial^2 A}{\partial x \partial y}\right|_{(x,x,x)} = 1 + f(x) + 2xf'(x) - x\theta.$$

The value of λ_ξ can be determined by inspection of figure 3. Additional information can be obtained from the condition that the trace of a matrix must be equal to the sum of its eigenvalues. This gives us

$$\lambda_\xi + 2\lambda_\zeta = 3x^2 f(x).$$

Since $f(x)$ is a monotonically increasing function the RHS is always negative. This allows us to deduce that (i) none of the stationary points along the $x = y = z$ line is a minimum since that would require both λ_ξ and λ_ζ to be positive and (ii) if λ_ξ is positive then λ_ζ must be negative.

6. Growth of nuclei

In this section we present both analytic and numerical investigations of the possible growth forms produced by the free energy given in equation (1). We find that a cubic growth morphology is always possible, but depending on the exact form of $f(x)$ a platelet growth morphology may also be possible. We use a simple model in which the growth rate of each face of the nucleus is proportional to the decrease in the free energy caused by that growth.

For a nucleus of sides x, y, z we can define a growth vector field $\boldsymbol{G}(x, y, z)$. This vector is given by

$$\boldsymbol{G} = \left(\frac{\mathrm{d}x}{\mathrm{d}t} \frac{\mathrm{d}y}{\mathrm{d}t} \frac{\mathrm{d}z}{\mathrm{d}t}\right).$$

$\boldsymbol{G}$ gives the rate at which the crystal grows in each direction. We choose a simple form for $\boldsymbol{G}$ in which the growth rate of the crystal depends on the free energy gradients and the size of the faces

$$\boldsymbol{G} \propto \left(-\frac{1}{yz}\frac{\partial A}{\partial x} - \frac{1}{zx}\frac{\partial A}{\partial y} - \frac{1}{xy}\frac{\partial A}{\partial z}\right).$$

Units of time can be chosen so that the constant of proportionality is unity.

$$\mathbf{G} = \left(-\frac{1}{yz}\frac{\partial A}{\partial x} - \frac{1}{zx}\frac{\partial A}{\partial y} - \frac{1}{xy}\frac{\partial A}{\partial z} \right).$$

This growth model is based on the idea that a system evolves in such a way as to locally decrease its free energy. This is the same idea that underlies the idea of nucleation, i.e. a pre-critical nucleus is one which can locally lower its free energy by dissolving and a post-critical nucleus is one which can locally lower its free energy by growing.

Using this equation for $\mathbf{G}$ we consider the possible outcomes of the growth of a nucleus; these outcomes are summarized in table 3. The possible outcomes we consider are dissolution, needle growth, growth into platelets and the growth of macroscopic cubes. We find that needle growth is always impossible and cubic crystal growth can always occur. Whether nuclei can dissolve or grow into platelets depends on the form of $f(x)$ near $x = 0$. One other possibility that we can immediately discount is that nuclei stop growing at some finite size. For this to be the case we must find a local minimum in $A(x, y, z)$. However if $f(x)$ is a monotonically increasing function then we can prove that no such minima exist. The condition for a minimum is that once a stationary point has been found and the quadratic expansion about that minimum has been diagonalized then the three diagonal elements must all be positive. This can be shown to be impossible since the trace of a matrix is invariant on changes of the co-ordinate system. Using this we can write

$$\lambda_1 + \lambda_2 + \lambda_3 = \frac{\partial^2 A(x, y, z)}{\partial x^2} + \frac{\partial^2 A(x, y, z)}{\partial y^2} + \frac{\partial^2 A(x, y, z)}{\partial z^2}$$

$$= \frac{\partial^2 f(x)}{\partial x^2} + \frac{\partial^2 f(y)}{\partial y^2} + \frac{\partial^2 f(z)}{\partial z^2}$$

where λ_1, λ_2 and λ_3 are the diagonal elements of the diagonalized matrix, i.e. the eigenvalues of the matrix. Since $f(x)$ is a monotonically increasing function its second derivatives are negative definite. Therefore the sum of the three eigenvalues must be negative so it is impossible that the three eigenvalues can all be positive.

To find out whether small nuclei dissolve or not we consider the behaviour of $\mathbf{G}$ for $x, y, z \to 0$. In this limit $\mathbf{G}$ is given by

$$\mathbf{G} = -(1 + f(0))\left[\frac{1}{y} + \frac{1}{z}\frac{1}{x} + \frac{1}{z}\frac{1}{x} + \frac{1}{y} \right].$$

If $1 + f(0) > 0$ then small nuclei dissolve because they have not reached a critical size. This is consistent with nucleation and growth theory. If however $1 + f(0) < 0$ then small nuclei grow instead of dissolving. The reason for this is that in this case the surface energy of a small nucleus is negative due to the surface relaxation contribution so it cannot provide a barrier to nucleation.

To find out whether cubic nuclei can form we consider $\mathbf{G}$ in the limit $x, y, z \to \infty$. This gives us

$$\mathbf{G} = \theta[1\,1\,1]$$

so large cubic nuclei are always stable, irrespective of the form of $f(x)$.

Next we consider the stability of a platelet nucleus. To do this we investigate the form of $\mathbf{G}$ for $x, y \to \infty$ and $z \to 0$. In this case we have

$$\mathbf{G} = -\left[\frac{1 + f(0)}{z}\frac{1 + f(0)}{z}f'(0) - \theta \right].$$

The conditions for platelets to be stable are $1 + f(0) < 0$ and $f'(0) - \theta > 0$. The first condition means that the surface energy for platelets must be negative. This means that the large surface

Table 3. Here we summarize the possible fates of a small crystal nucleus depending on the form of $f(x)$. A cubic growth morphology is always stable. Small nuclei dissolve if their surface energy is positive but cannot dissolve if it is negative. Platelets are stable if the surface energy of a thin platelet is negative and if the platelet cannot decrease its free energy by becoming thicker. Note: these conditions for determining possible growth morphologies are not entirely the same as the conditions determining the number of stationary values along the $x = y = z$ line summarized in table 2.

Possible morphologies	Condition(s)
Cubes or dissolve	$1 + f(0) > 0$
Cubes or platelets	$1 + f(0) < 0$
	$f'(0) - \theta > 0$
Cubes only	$1 + f(0) < 0$
	$f'(0) - \theta < 0$

area of a platelet is thermodynamically desirable. The second condition can be understood by considering the change in the free energy of a platelet on an increase in thickness. The surface energy will increase, not because of the change in surface area but because of the change in thickness. The bulk free energy will decrease because of the increase in volume. The second condition for the stability of the platelet requires that the increase in surface energy must be larger than the decrease in bulk energy.

Finally we consider the stability of needle shaped nuclei. To do so we look at the form of G for $z \to \infty$, $x, y \to 0$. Then we have

$$G = -(1 + f(0)) \left[\frac{1}{y} \frac{1}{x} \frac{1}{x} + \frac{1}{y} \right].$$

If $1 + f(0) > 0$ then needles become shorter and eventually dissolve. If $1 + f(0) < 0$ then needles become fatter and eventually become either platelets or cubes. We can also discount the possibility of needles with a large cross sectional area. The condition for these to be stable is that there is a minimum in $A(x, y, \infty)$. The same arguments that were used above to show that there were no minima in $A(x, y, z)$ can be used to show that there are no minima in $A(x, y, \infty)$.

These results show that it is the form of $f(x)$ near $x = 0$ that determines growth morphologies. This means that the surface relaxation contribution to $f(x)$, rather than the polarization contribution, is important in determining growth morphologies.

For more insight into how nuclei grow under the influence of a size dependent surface energy we plot numerical results for the growth field G using the free energy

$$A(x, y, z) = xy + yz + zx - \eta(xy\,e^{-z} + yz\,e^{-x} + zx\,e^{-y}) - \theta xyz.$$

$f(x)$ only has contributions from surface relaxations but we have demonstrated above that polarization contributions do not affect growth morphologies. In this case $f(x) = -\eta\,e^{-x}$ and $f(0) = -f'(0) = -\eta$. We plot G for three cases. Firstly we have $\eta = 0.5$, $\eta = 1$. In this case the possible outcomes of growth are cubes and dissolution. There are two stationary points on the $x = y = z$ line. Secondly we have $\eta = 5$, $\eta = 0.7$. The possible outcomes of growth are platelets and cubes. There are three stationary points along the $x = y = z$ line. Thirdly we have $\eta = 5$, $\eta = 1.2$. As before the possible fates of a crystal nucleus are cubes and platelets. However we only have one stationary point along the $x = y = z$ line. These three cases by no means exhaust the possible topologies of the growth field.

$G(x, y, z)$ is a three-dimensional vector field in a three-dimensional space. This makes it very difficult to represent on a two-dimensional piece of paper. In order to do so we take three slices through the field. The space in which the field exists represents the x, y and z
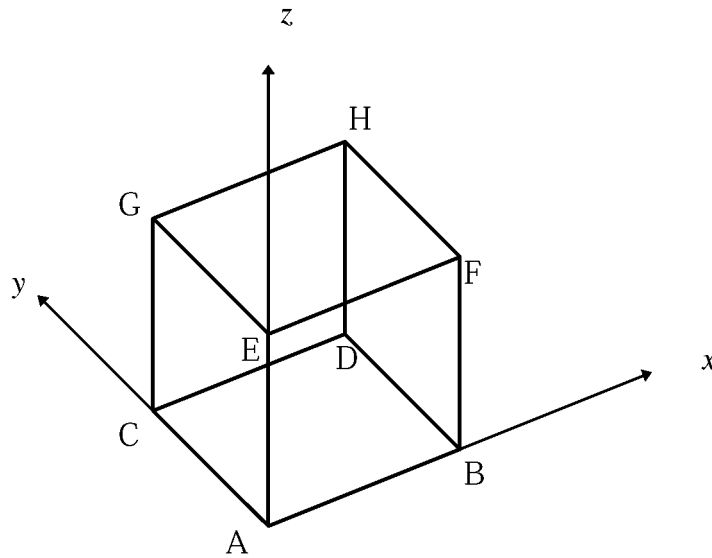
Figure 4. The growth field of a nucleus is a three-dimensional vector field in a three-dimensional space. It is very difficult to represent such a field on a two-dimensional piece of paper. In order to obtain an idea of the field we take slices of it. That is we take a plane, calculate the field on that plane and project the vectors onto that plane. The planes we have chosen are (i) ADHE which corresponds to cubic nuclei, (ii) ABDC which corresponds to very thin, platelet nuclei and (iii) EFHG which corresponds to very thick nuclei. In figures 5 to 7, part (a) shows the growth field projected onto the plane AEHD, part (b) shows the growth field projected onto the plane ABDC and part (c) shows the growth field projected onto the plane EFHG.

dimensions of the parallelepiped nuclei. These slices correspond to only considering certain shapes of nuclei. Firstly we take a slice corresponding to cuboid nuclei $x = y$. Secondly we look at platelet nuclei $z = 0.3$. Lastly we consider very thick nuclei $z = 4.5$. We calculate the growth field on these planes, then project the vectors obtained onto the plane. The resulting two-dimensional vectors are then normalized. Taken together these slices allow us to picture the vector field and allow us to determine the nature of stationary points.

In figure 4 the three planes described above are ABDC, AEHD and EFHG. On the diagram the point A is at co-ordinates $(0.3, 0.3, 0.3)$ and the point H is at co-ordinates $(4.5, 4.5, 4.5)$. In each of the cases considered the point H lies beyond all the stationary values of the $x = y = z$ line. Figures 5–7 show the growth field plotted in for the three cases described above. The letters at the corners of the plots are the same as those in figure 4.

Figure 5 corresponds to the usual nucleation and growth picture. Small nuclei dissolve, but sufficiently large nuclei grow into macroscopic cubes. Consider first figure 5(a). This shows the growth field for nuclei which are constrained to be cuboidal $(x = y \neq z)$. Point A corresponds to a small cubic nucleus of side length 0.3λ. Point D corresponds to a square platelet of thickness 0.3λ and breadth 4.5λ. Point E is a thin needle of length 4.5λ with a square base of side 0.3λ. Point H is a large cubic nucleus of side length 4.5λ. The line AH corresponds to cubic nuclei of increasing size. The line AE corresponds to square platelets of the same thickness but increasing breadth, beginning at A as very small cubes. The line EH corresponds to square platelets of increasing thickness ending up at H as large cubes. The line AE corresponds to needles of increasing height but the same base size, beginning at A as small cubes. The EH line corresponds to square based needles, with the base increasing in size until the nucleus becomes a cube at H. Along the line ED the needle nucleus decreases in height

E   H   C   D

A   D   A   B

(a)   (b)

G   H

E   F

(c)
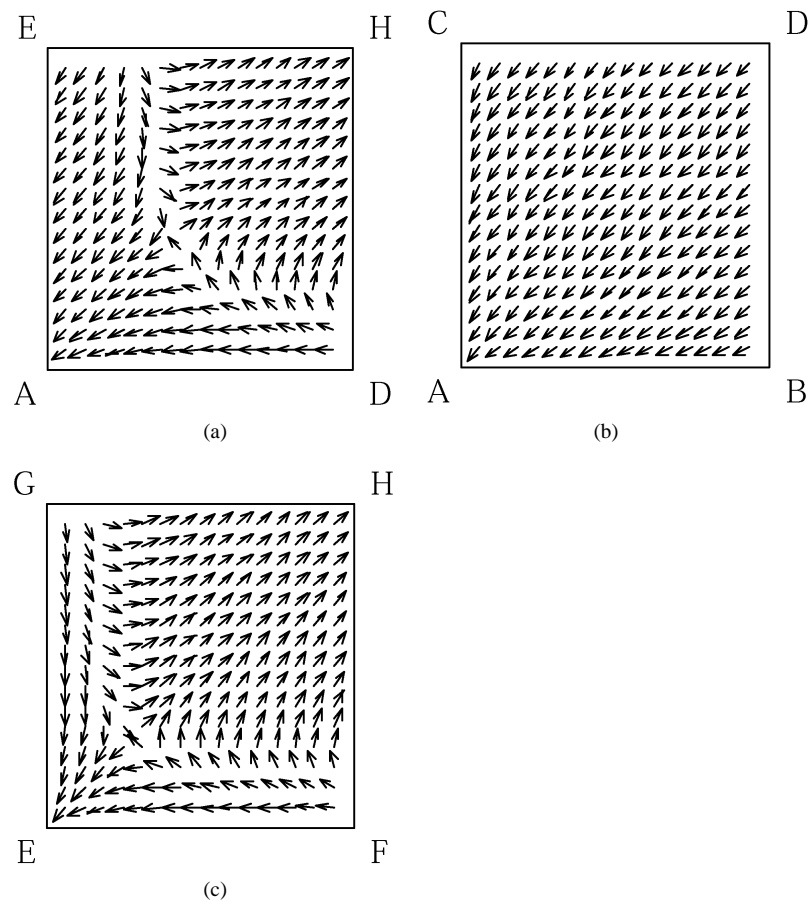
Figure 5. $\eta = 0.5, \theta = 1$. (a) This plot shows a typical nucleation and growth picture. Only nuclei in the top right part of the diagram tend to grow. These form large cubic crystals. Other nuclei dissolve. The saddle point approximately in the centre corresponds to the maximum in figure 3(a). Thin needles dissolve, thin platelets seem only to dissolve if they are small enough. Large platelets grow into cubic crystals. (b) This plot shows that the broad faces of platelets tend to shrink, which is what we expect from the previous diagram. The smaller platelet nuclei dissolve away entirely, but the larger nuclei thicken while their broad faces shrink and thus eventually become cubes. (c) Here again we see that nuclei that are thin needles dissolve but larger nuclei continue to grow.

and increases in base size. Half way along the line ED intersects the line AH and the nucleus is a cube. Past this point the nucleus height continues to decrease and its base continues to grow until it ends up as a platelet at H.

The arrows show the way in which the crystal would grow if it were constrained to remain as a cuboid as it grows. Looking along the cubic line, AH line the arrows change direction about one third of the way along. Arrows along the first third of the AH line point towards A, showing that small cubic nuclei tend to get smaller and dissolve. The arrows along the last two thirds of the AH line point towards H showing that sufficiently large nuclei tend to grow. This is consistent with the usual nucleation and growth picture. Close to the AE line the arrows point down left. This shows that needle shaped nuclei tend to shrink both in height and base size until they have dissolved. Close to the AD line the arrows point left showing that platelet nuclei tend to shrink in breadth. The arrows close to A are tilting downwards showing that the

(a)

(b)

(c)
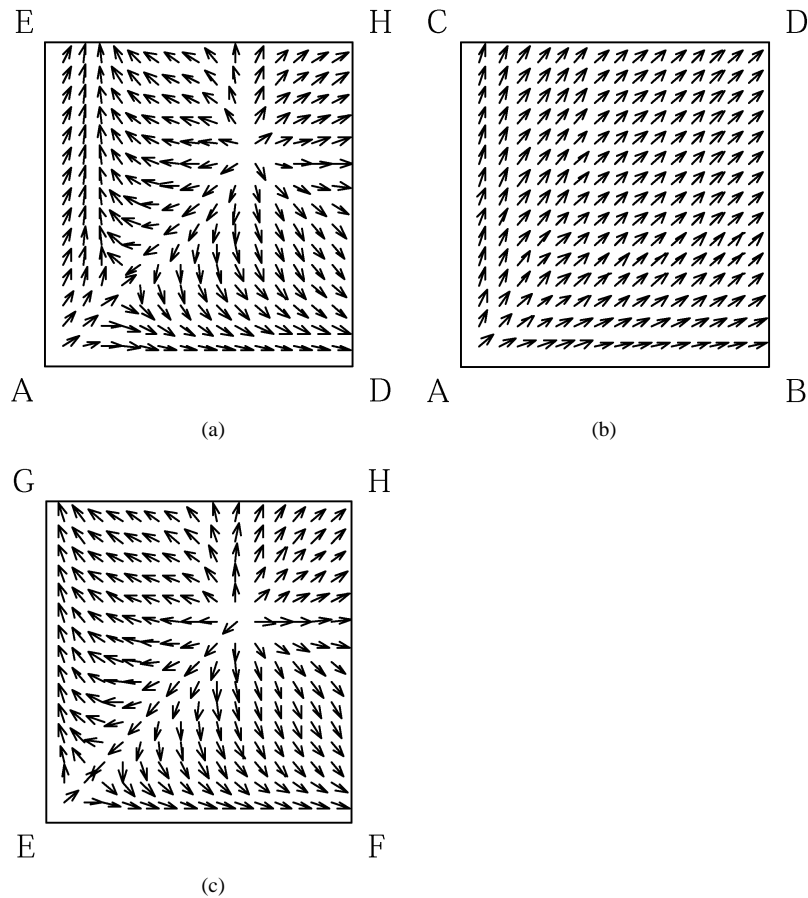
Figure 6. $\eta = 5$, $\theta = 0.7$. (a) This plot shows a saddle point and a maximum on the $x = y = z$ line. (There is also a maximum at the origin.) These correspond to the minimum and maximum in figure 3(b). This graph shows three features. Firstly, for nuclei in the top right portion of the diagram, growth into large cubes as we saw before. Secondly, in the bottom right part of the diagram, we see the growth of platelets. Lastly in the top left part of the diagram we see the apparent formation of needles. However plot (c) shows that these needles grow into platelets. (b) This plot shows that the broad faces of platelets tend to grow, so that they will eventually become square platelets. (c) The saddle point in the bottom left corner corresponds to the needles seen in part (a). This plot shows that the needles will grow into platelets. The maximum approximately in the centre shows the growth of cubes.

thickness of platelet nuclei decreases as well. These nuclei will dissolve. Arrows closer to D are tilted upward slightly showing that as the breadth of the nuclei decreases their thickness increases. Following the path of the arrows shows that these nuclei will grow into macroscopic cubes.

Figure 5(b) shows the growth field for the case of very thin nuclei ($z = 0.3\lambda$). Point A is the same as that in figure 5(a), i.e. a small cubic nucleus edge length 0.3λ. Point D again is the same as in figure 5(a), i.e. a thin platelet of breadth 4.5λ and thickness 0.3λ. Points B and C both represent thin needles with square bases. The needles have a height of 4.5λ and the base has an edge length of 0.3λ. The AB and AC lines are exactly the same as the AE line in figure 5(a). The lines BD and CD are however not the same as the line ED in figure 5(a).
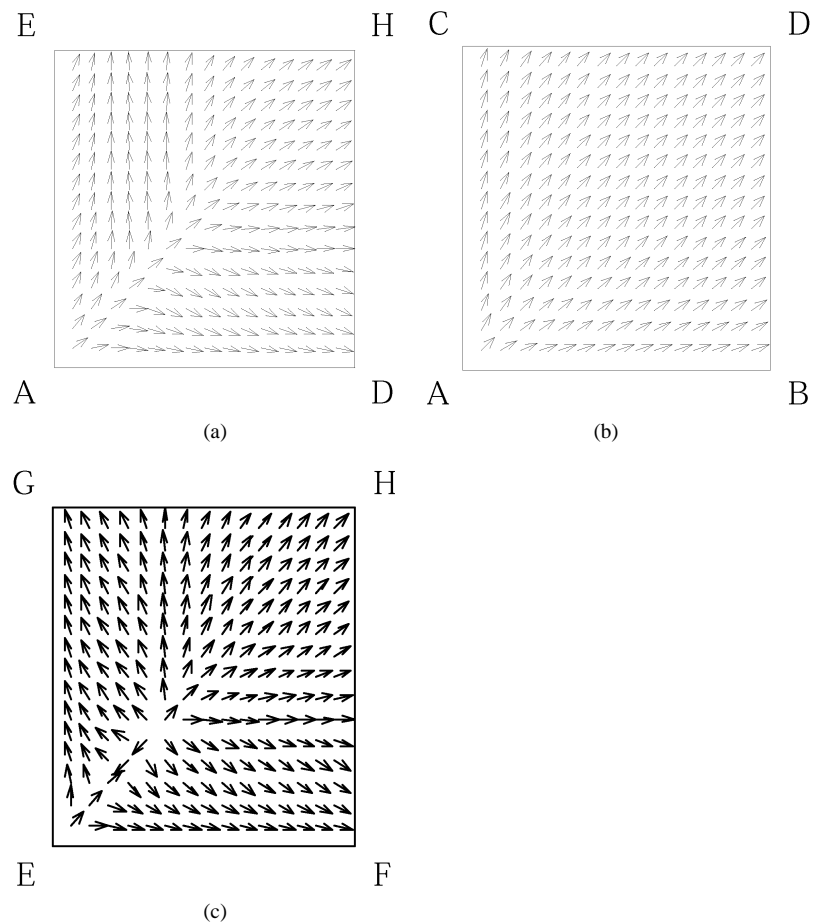
Figure 7. $\eta = 5$, $\theta = 1.2$. (a) This plot does not show the maximum and saddle point of the previous case. However it does still show the other features of the previous plot, that is platelet and cube growth as well as apparent needle growth which as before turns out to be unstable with respect to platelet growth. (b) This plot shows that platelets still grow as in the previous case. (c) As before this plot shows that needle growth is unstable with respect to the formation of platelets.

Although along both paths a needle turns into a platelet the transformation between the two is different. Along the path ED the height of the needle decreases while the edge length of its square base increases. Along the paths BD and CD the height of the needle remains the same but one edge of its base increases. Eventually this edge of the base is as large as the height of the original needle and we have a platelet.

All the arrows in this plot point down and left showing that platelet and needle nuclei tend to shrink. However as we saw in figure 5(a) large platelet nuclei thicken as their large face shrinks. That means that this graph cannot be interpreted as all platelet and needle shaped nuclei dissolving because the growth field has an extra dimension.

In figure 5(c) point E is the same as point E in figure 5(a) and corresponds to a square based needle. Point H is again the same as in figure 5(a) and corresponds to a cube, edge length 4.5λ. Points F and G both correspond to square based platelets. The lines EF and EG are equivalent to the lines BD and CD in figure 5(b). Along lines FH and GH the thickness of the platelets increases until the platelets have turned into cubes.

The arrows along the EF and EG lines point towards E, suggesting that platelets tend to turn into needles. However we know from figure 5(a) and (b) that in fact platelets tend to shrink into less broad platelets so what we are seeing here is an artefact from projecting the three-dimensional growth field onto a two-dimensional plane. All the arrows in the top right of the plot are pointing in the general direction of H showing that these nuclei tend to grow.

In this case we could have formed a good idea of what the growth field looks like just from considering figure 5(a). However for the systems in which surface relaxations are large shown in figure 6 and figure 7 this is not the case. For instance in figure 6(a), close to the AE line we see a line of arrows pointing directly up. This suggests that we have needles of constant base size growing in height. But looking at figure 6(c) we see that these needles are unstable and grow into platelets.

The plots in figure 6 show a departure from the growth morphology predicted by the Wulff plot. Although sufficiently large nuclei form cubic crystals as in the case then the surface relaxation is unimportant (figure 5), we also see that nuclei which would have dissolved now grow into platelets. In this case the stability of the cubic line has changed. As before large cubic nuclei are stable. However small cubic nuclei are unstable. Small nuclei now grow into platelets, whether they started off as needles, platelets or cubes. There are no nuclei that dissolve. We interpret this as meaning there is no nucleation barrier to the formation of platelets. These flow diagrams show that the minimum in figure 3(b) cannot be interpreted as the stabilization of small nuclei. The diagrams show that the minimum is in fact a saddle point.

The plots in figure 7 show much the same behaviour as the plots in figure 6, except along the $x = y = z$ line. The outcomes are the same: nuclei end up as either cubes or platelets. Again for small nuclei the cubic line is unstable. Figure 3(c) cannot be interpreted as all nuclei growing into macroscopic cubes with no nucleation barrier. Instead, as before, small nuclei grow into platelets.

7. Numerical estimates

We now need to address the question of whether this effect can occur in practice. In this work we do not attempt to find a material in which this mechanism for platelet growth occurs but merely to demonstrate the possibility that such a material may exist. That is, we look at the values of the parameters of the surface relaxation and the surface energy needed to produce platelet growth and consider if they are comparable with those found in real materials. We considered the perovskite class of materials, in which surface relaxations are known to be significant. We considered the perovskite materials lead titanate ($PbTiO_3$), strontium titanate ($SrTiO_3$), barium titanate ($BaTiO_3$) and lanthanum aluminate ($LaAlO_3$). These materials all have zigzag relaxations: $q > 0$ and $Q > 0$. Out of the two conditions that need to be met for platelet formation to take place, the second $\eta > \theta$ can always be met by growing the crystals with a small enough degree of supersaturation or supercooling. The first condition $\eta > 1$ depends on the relative sizes of the surface interaction term and the constant term in the surface energy. By considering the size of the surface relaxations and the surface energies in perovskite materials we show that the effect may occur in practice. The results of this section do not demonstrate that we can expect platelet growth to occur in any of the materials considered. What they do show is that the effect described above cannot be ruled out as impossible for real materials.

As we showed in the previous section the parameter which determines whether equilibrium platelet growth is feasible is η. This parameter must have a value higher than one for equilibrium platelet growth to occur. η is the ratio of the prefactor of the exponential term in the free energy

to the surface energy. In the notation of the section on surface relaxations the equation for η is:

$$\eta = \frac{2Q^3(2b-A)^2}{\sigma\lambda(q+Q/\lambda)^2 b^2}$$

for the zigzag case where σ is the surface energy, and λ is dimensionless as it is measured in unit cell lengths.

We estimated the various quantities from data in the literature. Chrosch and Salje (1998) give values of λ for the above compounds. From these values, the lattice parameters b and the C_{1111} elastic constants we obtained Q and q. We calculated $(2b - A)$ from the strain in the first layer, which is given by

$$\left(\frac{u}{b}\right)_{first\ layer} = \left(\frac{Q}{q+Q/\lambda}\right)\frac{2b-A}{B}$$

for a system much larger than λ (see appendix A). As a lower limit on the surface energy σ, we used the energy per unit area of a twin domain wall. We summarize these results in table 4.

Table 4. Values of η for various perovskites. We could not find all the data we needed so some values had to be interpolated from their values in other compounds. Only strontium titanate has an η value large enough for platelet formation to take place. This is due to its very low value for σ.

	$PbTiO_3$	$SrTiO_3$	$BaTiO_3$	$LaAlO_3$
λ	1.26[a]	1.55[b]	3.50[c]	5.00[d]
b (10^{-10} m)	3.96	4.00	4.00	3.80
C_{1111} (10^{11} Pa)	3.00[e]	3.48[f]	2.75[f]	3.00[e]
Q (N m^{-1})	25.66	31.54	26.96	28.22
q (N m^{-1})	16.16	13.13	2.20	1.13
ε (%)	2.00[e]	2.00[e]	2.00[g]	2.00[e]
$(2b-A)/b$ (%)	2.85	2.12	0.73	0.48
σ (10^{-3} J m^{-2})	50.00[a]	1.30[d]	10.00[d]	28.00[d]
η	0.33	12.52	0.62	0.16

[a] Stemmer *et al* (1995).
[b] Cao and Barsch (1990).
[c] Tsai *et al* (1992).
[d] Chrosch and Salje (1999).
[e] Estimated from values for other materials in the table.
[f] Lide (1997).
[g] Padilla and Vanderbilt (1997).

Table 4 shows that only strontium titanate has an η value large enough for platelet formation to take place. However the values for $PbTiO_3$ and $BaTiO_3$ are not far away from the critical value. This suggests that the effect reported here may occur in actual materials. The σ values we are using are those of twin domain walls rather than free surfaces. A calculation of the free surface energy of YBCO at 0 K gave 800 mJ m^{-2} (Granzio and Uccio 1997). This is much higher than the values given in the table. There are many factors that can bring this surface energy down. The phonon contribution to the surface free energy can significantly reduce it as we show in section 2. In crystallization we are usually dealing with a crystal in contact with a solution or its melt, and this may reduce the surface energy substantially. A reconstruction of the surface will also lower its free energy. We also expect that the surface relaxation may be made larger by a layer of impurity atoms on the surface, which will alter the boundary conditions of the surface relaxation equations.

8. Conclusions

We have shown that surface relaxations and polarization fluctuations modify the surface energies of small nuclei, producing an effective surface energy. This effective surface energy depends on the separation between surfaces. For systems with large surface relaxations the effective surface energy may be negative for very thin platelets. If this is the case then we predict that the small nuclei will grow into platelets. These growth forms are not predicted by the Wulff plot, which only determines the growth morphology of large nuclei. Lastly since the effective surface energy of platelets is negative the surface energy will not be a nucleation barrier to their formation.

Acknowledgments

Appendix A. Calculation of surface relaxation energy

The notation used in this section is explained in figure 2. Here we calculate the results presented in section 4.

Firstly we consider the case $Q < 0$. The potential energy of the system is

$$V = \frac{q}{2} \sum_{n=0}^{N} (\Delta_n - a)^2 + \frac{Q}{2} \sum_{n=0}^{N-1} (\Delta_n + \Delta_{n+1} - A)^2.$$

We find the minimum in the potential energy as the solution to the equations

$$\frac{\partial V}{\partial \Delta_n} = 0 \qquad n = 0, 1, \ldots, N.$$

This gives us the following equations to solve

$$0 = q(\Delta_0 - a) + Q(\Delta_0 + \Delta_1 - A) \tag{A1}$$

$$0 = q(\Delta_m - a) + Q(\Delta_{m-1} + 2\Delta_m + \Delta_{m+1} - 2A) \qquad m = 2, 3, \ldots N - 1 \tag{A2}$$

$$0 = q(\Delta_N - a) + Q(\Delta_{N-1} + \Delta_N - A). \tag{A3}$$

In this case there is an exponentially decaying relaxation (Houchmandzadeh *et al* 1992). We assume that the displacements associated with the relaxation vary slowly enough that a continuum approximation can be made, i.e.

$$\Delta_n = b + u(x_n)$$

where b is the lattice parameter in the bulk

$$b = \frac{qa + 2QA}{q + 4Q} \tag{A4}$$

and $u(x)$ is a slowly varying function of x, with

$$x_n = -\frac{N}{2} + n.$$

Equation (A2) becomes a differential equation for u

$$Q\frac{\partial^2 u}{\partial x^2} + (q + 4Q)u = 0.$$

Equation (A1) and equation (A3) give boundary conditions for u.

$$(q + 2Q)u\left(-\frac{N}{2}\right) + Qu'\left(-\frac{N}{2}\right) = \frac{1}{2}Q(2b - A) \tag{A5}$$

$$(q + 2Q)u\left(\frac{N}{2}\right) - Qu'\left(\frac{N}{2}\right) = \frac{1}{2}Q(2b - A). \tag{A6}$$

In fact only one of these boundary conditions is necessary since the symmetry of the system requires that $u(x)$ is an even function of x, i.e. $u(x) = u(-x)$. The only solution of the differential equation with the correct symmetry is

$$u(x) = \Gamma \cosh\left(\frac{x}{\lambda}\right)$$

where Γ is to be determined by the boundary conditions, and λ, the relaxation length scale, is given by

$$\lambda = \sqrt{\frac{-Q}{q + 4Q}}.$$

The condition that u is a slowly varying function of x can now be stated as $\lambda \gg 1$.

We calculate Γ from the boundary condition equation (A5)

$$\Gamma = \frac{Q(2b - A)}{[(q + 2Q)\cosh(N/2\lambda) - Q/\lambda \sinh(N/2\lambda)]}.$$

Now we expand Γ in a power series in the parameter ξ, where

$$\xi = \exp\left(\frac{N}{2\lambda}\right).$$

This gives us

$$\Gamma = \frac{2Q(2b - A)}{[q + 2Q - Q/\lambda]\xi}\left[1 - \left(\frac{q + 2Q + Q/\lambda}{q + 2Q - Q/\lambda}\right)\frac{1}{\xi^2}\right] + O\left(\frac{1}{\xi^5}\right).$$

Now we use these results to calculate the potential energy of the system in terms of u. First we expand the potential energy in powers of u. Since u is very small (strains are in practice of the order of 1%; see for example Padilla and Vanderbilt 1997) we can discard the term that is second order in u.

$$V = \frac{q}{2}\sum_{n=0}^{N}(b + u(x_n) - a)^2 + \frac{Q}{2}\sum_{n=0}^{N-1}(2b + u(x_n) + u(x_{n+1}) - A)^2$$

$$V = \frac{q}{2}N(b - a)^2 + \frac{Q}{2}(N - 1)(2b - A)^2 + q(b - a)\sum_{n=0}^{N}u(x_n)$$

$$+ Q(2b - A)\sum_{n=0}^{N-1}(u(x_n) + u(x_{n+1})) + O(u^2).$$

The first two terms are the potential energy of the unrelaxed system so these constitute the bulk energy V_B. Using equation (A4) we can eliminate many of the terms from the expansion of $V - V_B$.

$$V - V_B = [q(b - a) + Q(2b - A)](u(x_0) + u(x_N)) + [q(b - a) + 2Q(2b - A)]\sum_{n=1}^{N-1}u(x_n)$$

$$V - V_B = [q(b - a) + Q(2b - A)](u(x_0) + u(x_N))$$

$$V - V_B = -Q(2b - A)(u(x_0) + u(x_N))$$

$$V - V_B = -2Q(2b - A)u(x_0).$$

The last line follows from the symmetry of u. We substitute for $u(x_0)$ and expand in powers of ξ.

$$V - V_B = -2Q(2b - A)\Gamma \cosh\left(\frac{N}{2\lambda}\right)$$

$$V - V_B = -Q(2b - A)\Gamma\left(\xi + \frac{1}{\xi}\right).$$

Lastly we substitute for Γ

$$V - V_B = -\frac{2Q^2(2b - A)^2}{[q + 2Q - A/\lambda]\xi}\left[1 - \left(\frac{q + 2Q + Q/\lambda}{q + 2Q - Q/\lambda}\right)\frac{1}{\xi^2}\right]\left(\xi + \frac{1}{\xi}\right)$$

$$V - V_B = -\frac{2Q^2(2b - A)^2}{[q + 2Q - A/\lambda]} + \frac{4Q^3(2b - A)^2}{\lambda[q + 2Q - Q/\lambda]^2\xi^2} + O\left(\frac{1}{\xi^4}\right).$$

This gives us the result given in section 2:

$$V - V_B = -\frac{2Q^2(2b - A)^2}{[q + 2Q - Q/\lambda]} + \frac{4Q^3(2b - A)^2}{\lambda[q + 2Q - Q/\lambda]^2} \exp\left(-\frac{N}{\lambda}\right).$$

Next we consider the case $Q > 0$. In this case as before we obtain the equations (A1)–(A3). Also the lattice parameter b is given by the same equation as before. However the relaxation in this case is a zigzag relaxation. The lattice alternately expands and contracts but with an overall exponential envelope. For this reason we cannot define u in the same way as before because in this case it would not be a slowly varying field and our continuum approximation would not be valid. Instead we define u by

$$\Delta_n = b + (-1)^n u(x_n).$$

Now u is a slowly varying function of x because we have taken the zigzag part of the relaxation out. The x_n are defined as before. We can deduce the symmetry of $u(x)$ from the symmetry of the system. The system has inversion symmetry about its centre. That is

$$\Delta_{N/2+i} = \Delta_{N/2-i}.$$

This means that u must be an even function if N is even and an odd function if N is odd. As before we obtain a differential equation for u.

$$qu - Q\frac{\partial^2 u}{\partial x^2} = 0.$$

This has solutions

$$u = \Gamma \cosh\left(\frac{x}{\lambda}\right) \qquad N \text{ even}$$

$$u = \Gamma \sinh\left(\frac{x}{\lambda}\right) \qquad N \text{ odd}$$

$$\lambda = \sqrt{\frac{Q}{q}}.$$

The solutions for u are different depending on whether N is odd or even because u has different symmetries in these two cases. Apart from this the calculation proceeds in the same way as before but with the new definition of u.

The result for the potential energy is

$$V - V_B = -\frac{2Q^2(2b - A)^2}{[q + A/\lambda]} - (-1)^N \frac{4Q^3(2b - A)^2}{\lambda[q + Q/\lambda]^2} \exp\left(-\frac{N}{\lambda}\right).$$

We assume that during crystal growth the system only experiences the (negative) envelope.

Appendix B. The effect of phase transitions on η and λ

In this section we consider how a ferroelastic phase transition affects the value of the parameter η. We show that as the system is cooled to T_C from above η decreases to zero. This result makes sense because as mentioned before as $T \to T_C$, $\lambda \to \infty$. The surface relaxation goes all the way through the material. It is no longer a surface effect but a bulk effect. The contribution it makes to the surface energy must therefore be zero. This means that platelet formation, which requires $\eta > 1$, will not take place at temperatures near ferroelastic transitions.

Near a phase transition some of the parameters of the system shown in figure 2 above will depend strongly on temperature. As we mentioned in section 2 our model has instabilities that correspond to ferroelastic phase transitions. The stability conditions are $Q > -q/4$ and $q > 0$. These conditions are explained by a calculation of the phonon spectrum of the system by Houchmandzadeh *et al* (1992).

$$\omega^2 = q \sin^2(\tfrac{1}{2}kb) + Q \sin^2(kb)$$

where k is the (one-dimensional) phonon wavevector.

To see how the parameters η and θ are affected by phase transitions consider the case where $Q > 0$. We consider the system in the region where the temperature is close to T_C but above it. In a soft mode phase transition the frequency of the soft mode has temperature dependence

$$\omega^2 \propto (T - T_C)$$

(Dove 1997). With $Q > 0$ the mode that softens is the one at $kb = \pi/2$. This mode has $\omega^2 = q$. So q must have the temperature dependence

$$q \propto (T - T_C).$$

This condition is the only one necessary for a phase transition so we can assume that all the other parameters of the model vary more slowly than q in the region of T_C. That is Q, σ, a, A do not, to first approximation, vary in the region of T_C. However λ and b are both functions of q so these also depend on $(T - T_C)$. We calculate the behaviour of η in the region of T_C first. η is given by

$$\eta = \frac{2Q^3(2b - A)^2}{\sigma \lambda (q + Q/\lambda)^2 b^2}.$$

The temperature dependence of the parameters q, λ and $(2b - A)$ is given by

$$q = \bar{q}t$$
$$\lambda = \bar{\lambda}t^{-1/2}$$
$$b = \frac{1}{2}(2a - A)\bar{q}t + \frac{A}{2}$$

where

$$t = \frac{T - T_C}{T_C}.$$

By substituting these into the equation for η we obtain its temperature dependence.

$$\eta = \frac{2Q^3((2a - A)/4Q)^2 \bar{q}^2 t^2}{\sigma \bar{\lambda} t^{-1/2}(\bar{q}t + Q/\bar{\lambda}t^{-1/2})^2(A/2)^2}$$
$$\eta = \frac{Q\bar{q}^2(2a - A)^2}{8\sigma \bar{\lambda}(\bar{q}t^{1/2} + Q/\bar{\lambda})^2(A/2)^2}t^{3/2}$$
$$\lim_{t \to 0} \eta \propto t^{3/2}.$$

So η becomes very small as we approach the transition temperature. These equations are of course only valid for $T > T_C$. Below T_C the structure is different and all the parameters will have different values. σ has a contribution from the surface relaxation, but it decreases to zero as we approach the transition temperature.

The t dependence of θ can be written down almost immediately:

$$\theta = \frac{r^*}{2\lambda}$$
$$\theta = \frac{r^*}{2\bar{\lambda}t^{-1/2}}$$
$$\theta \propto t^{1/2}.$$

So θ becomes very small as we approach the transition temperature. This means that the bulk free energy xyz/θ will be very large. This makes sense because x, y, z are measured in units of λ which is also very large near the transition temperature. The free energy per unit volume θ^{-1} becomes very large because the unit volume is also very large.

References

Baidakov V G and Boltachev G Sh 1999 Curvature dependence of the surface tension of liquid and vapour nuclei *Phys. Rev.* E **59** 469–75

Bögels G, Meeks H, Bennema P and Bollen D 1999 Twin formation and morphology of vapour grown silver halide crystals *Phil. Mag.* A **79** 639–53

Bögels G, Pot T M, Meeks H, Bennema P and Bollen D 1997 Side-face structure and growth mechanism of tabular silver bromide crystals *Acta Crystallogr.* A **53** 84–94

Cao W and Barsch G R 1990 Landau–Ginzburg model of interphase boundaries in improper ferroelastic perovskites of D_{4h}^{18} symmetry *Phys. Rev.* B **41** 4334–48

Chrosch J and Salje E K H 1999 The temperature dependence of the domain wall width in LaAlO$_3$ *J. Appl. Phys.* **85** 722–7

Dove M T 1993 *Introduction to Lattice Dynamics* (Cambridge: Cambridge University Press)

——1997 Silicates and soft modes *Amorphous Insulators and Semiconductors (NATO ASI Series 3. High Technology)* ed M F Thorpe and M I Mitkova (Amsterdam: Kluwer) vol 23, pp 349–83

Dove M T, Harris M J, Hannon A C, Parker J M, Swainson I P and Gambhir M 1997 Floppy modes in crystalline and amorphous silicates *Phys. Rev. Lett.* **78** 1070–3

Dove M T, Heine V and Hammonds K D 1995 Rigid unit modes in framework silicates *Mineral. Mag.* **59** 629–39

Giddy A P, Dove M T, Pawley G S and Heine V 1993 The determination of rigid-unit modes as potential soft modes for displacive phase transitions in framework crystal structures *Acta Crystallogr.* A **49** 697–703

Granasy L 1998 Semiempirical van der Waals/Cahn–Hilliard theory: size dependence of the Tolman length *J. Chem. Phys.* **109** 9660–3

Granzio F M and Uccio U S 1997 Simple model for the nucleation of (001) and (100) oriented grains in YBCO films *J. Cryst. Growth* **174** 409–16

Hammonds K D, Deng H, Heine V and Dove M T 1997 How floppy modes give rise to adsorption sites in zeolites. *Phys. Rev. Lett.* **78** 3701–4

Hammonds K D, Dove M T, Giddy A P and Heine V 1994 CRUSH: a FORTRAN program for the analysis of the rigid unit mode spectrum of a framework structure *Am. Mineral.* **79** 1207–9

Hammonds K D, Dove M T, Giddy A P, Heine V and Winkler B 1996. Rigid unit phonon modes and structural phase transitions in framework silicates *Am. Mineral.* **81** 1057–79

Hammonds K D, Heine V and Dove M T 1998 Rigid Unit Modes and the quantitative determination of the flexibility possessed by zeolite frameworks *J. Phys. C: Solid State Phys.* B **102** 1759–67

Hartman P (Ed) 1973 *Crystal Growth: an Introduction* (Amsterdam: North-Holland)

Houchmandzadeh B, Lajzerowicz and Salje E 1992 Relaxations near surfaces and interfaces for first-, second-, and third-neighbour interactions: theory and applications to polytypism. *J. Phys.: Condens. Matter* **4** 9779–94

Kalikmanov V I 1997 Semiphenomenological theory of the Tolman length *Phys. Rev.* E **55** 3068–71

Landau L D and Lifshitz E M 1980 *Statistical Physics* part 1 (Oxford: Butterworth-Heinemann)

Lide D R (ed) 1997 *CRC Handbook of Chemistry and Physics* 78th edn (New York: Chemical Rubber Company)

Lipowsky R 1985 Critical effects at complete wetting *Phys. Rev.* B **32** 1731–50

Lipowsky R 1987 Surface critical phenomena at first order phase transitions *Ferroelectrics* **73** 69–81

Padilla J and Vanderbilt D 1997 *Ab initio* study of BaTiO$_3$ surfaces *Phys. Rev.* B **56** 1625–31

Pluis B, Taylor T N, Frenkel D and Van der Veen J F 1989 Role of long-range interactions in the melting of a metallic surface. *Phys. Rev.* B **40** 1353–6

Pryde A K A, Dove M T and Heine V 1998. Simulation studies of ZrW$_2$O$_8$ at high pressure *J. Phys.: Condens. Matter* **10** 8417–28

Pryde A K A, Hammonds K D, Dove M T, Heine V, Gale J D and Warren M C 1996 Origin of the negative thermal expansion in ZrW$_2$O$_8$ and ZrV$_2$O$_7$ *J. Phys.: Condens. Matter* **8** 10973–82

Stemmer S, Streiffer S K and Ernst F 1995 Atomistic structure of 90° domain walls in ferroelectric PbTiO$_3$ thin films *Phil. Mag.* A **71** 713–24

Thorpe M F 1995 Bulk and surface floppy modes *J. Non-Crystal. Solids* **182** 135–42

Tolman R C 1949 The effect of droplet size on surface tension *J. Chem. Phys.* **17** 333–7

Trachenko K, Dove M T, Hammonds K D, Harris M J and Heine V 1998 Low-energy dynamics and tetrahedral reorientations in silica glass *Phys. Rev. Lett.* **81** 3431–4

Tsai F, Khiznichenko V and Cowley J M 1992 High-resolution electron-microscopy of 90° ferroelectric domain boundaries in BaTiO$_3$ and Pb(Zr$_{0.52}$Ti$_{0.48}$)O$_3$ *Ultramicroscopy* **45** 55–63

Welche P R L, Heine V and Dove M T 1998. Negative thermal expansion in β-quartz *Phys. Chem. Miner.* **26** 63–77

Widom B 1978 Structure of the $\alpha\gamma$ interface *J. Chem. Phys.* **68** 3878–83